Fluid Phase Equilibria 337 (2013) 119–124

Contents lists available at SciVerse ScienceDirect

Fluid Phase Equilibria

journal homepage: www.elsevier.com/locate/fluid

Thermal conductivity, rheological behaviour and density of non-Newtonian ethylene glycol-based SnO_2 nanofluids

Alejandra Mariano[a], María José Pastoriza-Gallego[b], Luis Lugo[b], Alberto Camacho[a], Salvador Canzonieri[a], Manuel M. Piñeiro[b,*]

[a] Facultad de Ingeniería, CONICET, Universidad Nacional del Comahue, Neuquén (8300), Argentina
[b] Departamento de Física Aplicada, Facultade de Ciencias, Universidade de Vigo, E-36310 Vigo, Spain

ARTICLE INFO

Article history:
Received 3 June 2012
Received in revised form
19 September 2012
Accepted 21 September 2012
Available online 28 September 2012

Keywords:
Nanofluid
Thermal conductivity
Rheology
Density
Tin(IV) oxide

ABSTRACT

The thermal conductivity, rheological behaviour and the high-pressure density of several non-Newtonian ethylene glycol-based SnO_2 nanofluids were analysed. The thermal conductivity and density were measured at 283.15, 303.15 and 323.15 K whereas rheological characterization was performed at 303.15 K. Nanofluids with concentrations of SnO_2 nanoparticles up to 25% in weight fraction were designed for thermal conductivity and rheological studies while density behaviour were analysed up to 5% at pressures up to 45 MPa. Thermal conductivity increases as usual with weight fraction showing an enhancement up to 14% in the range studied, and the experimental values were compared with available theoretical models. The volumetric behaviour shows a contractive behaviour and a departure from ideal behaviour, which is incremented with the concentration of the nanoparticles. The temperature and pressure dependence on this contractive behaviour is also studied. The rheological tests performed evidence shear thinning behaviour. In addition, the viscosity at a given shear rate is time dependent, i.e. the fluid is rheopectic. Finally, using strain sweep and frequency sweep tests the storage modulus, G', and loss modulus, G'', were determined, showing viscoelastic behaviour for all samples, a fact that must be carefully taken into account for any application involving nanofluid flow.

1. Introduction

The suspension of nanoscale particles in a fluid is a colloidal system usually referred to as nanofluid. In recent years it has been shown that adding nanoparticles to a fluid produces a very remarkable change on its thermophysical properties, including remarkable variations in its transport properties, far from the estimates obtained by classical theories of suspensions that work properly for larger particle sizes. This anomalous increase in properties such as thermal conductivity or viscosity is therefore associated to the system scale, determined by the size of the particles in suspension, and not only by its nature. This phenomenon has been reported for metallic nanoparticles, but also from those derived from metal oxides, ceramics, or carbon nanotubes.

The fact that, for instance, the thermal conductivity of a nanofluid largely exceeds the values expected for a classical colloid of the base fluid attracted in a first stage attention on their potential use for replacement of conventional heat exchange fluids [1–7]. The realization that this unusual enhancement on heat transport properties occurs even at low concentrations of nanoparticles has suggested an improvement in the performance of the cited working fluids by reducing its load in industrial applications. This was the leading reason that has made research on nanofluids an emerging field with many postulated practical applications in industry [3,8–10]. Moreover, it has been shown that other transport properties exhibit also unusual behaviour, including viscosity and other related rheological properties [11–15].

Nevertheless, there are still important discrepancies between different thermal conductivity data sets reported in literature for this type of systems, and this is believed to be due to the combination of several factors as the diversity of preparation processes, particle size dispersion, stability, non-uniformity of the particle shape, clustering, sedimentation or pH [3,7,16]. The production route from the nanoparticle synthesis and chemical and morphological characterization, dispersion techniques and determination of stability conditions, continuing to the experimental measurement procedure itself has raised doubts in certain cases concerning sample reproducibility and data reliability. Unfortunately much effort is still necessary in this direction, and special care must be taken in the detailed control and description of all variables involved in nanofluid sample preparation and handling.

* Corresponding author.
E-mail addresses: mmpineiro@uvigo.es, manumar@uvigo.es (M.M. Piñeiro).

0378-3812/$ – see front matter © 2012 Elsevier B.V. All rights reserved.
http://dx.doi.org/10.1016/j.fluid.2012.09.029

List of symbols

A	constant in Eq. (3)
D	nanoparticle diameter
G'	storage modulus
G''	loss modulus
V^E	excess specific volume
w	mass fraction

Greek symbols

ϕ	concentration in volume fraction
$\dot{\gamma}$	shear rate
η	viscosity
κ	thermal conductivity
λ	wavelength
ρ	density
ω	angular frequency (rad s^{-1})

Abbreviations

Abs	absorbance
UV–vis	ultraviolet–visible
wt%	concentration in mass percent

Subscripts

0	base fluid
nf	nanofluid

Some experimental studies on SnO_2 nanoparticles dispersed in different fluids have recently been published [17–20]. Data about rheological properties of tin oxide slurries dispersed with polyacrylic acid and polyvinylbutyral have been reported by dos Santos et al. [18]. More recent works, as the one carried out by Ahmari et al. [17], report electro rheological properties of non-Newtonian fluids (silicon oil) with the addition of SnO_2 nanoparticles finding that the apparent viscosity of suspensions increases with concentration of SnO_2 as well as electrical voltage. Habibzadeha et al. [19] studied the colloidal stability of SnO_2 nanofluids prepared by dispersing nanoparticles in deionized water as base fluid, using UV–vis spectrophotometric measurements. They found that after 500 h of sedimentation time the relative concentration of the nanofluid with the highest stability had reduced to 77% the initial value. Also, the authors measured the thermal conductivities of the nanofluid with a transient hot-wire apparatus and studied the effects of pH and temperature on the thermal conductivity finding a maximum thermal conductivity enhancement of up to 8.7% at 353 K for 0.024 wt% concentration.

The objective of this article is to study nanofluids composed by SnO_2 nanoparticles dispersed in ethylene glycol (EG), in a concentration up to 25% in weight fraction. The characteristics of the powder, stability, and size distribution are analysed and discussed. Then the transient hot-wire technique is used to determine the thermal conductivity and the effects of both volume fraction and temperature were evaluated, and the experimental values were compared with theoretical models proposed for thermal conductivity estimation. Moreover, these nanofluids were subjected to rheological analyses using a Physica MCR 101 Rheometer (Anton Paar, Austria) and the effect of volume fraction at a constant temperature was analysed. Finally, the volumetric behaviour of the nanofluids has been determined experimentally by measuring the density variation in a wide pressure and temperature range.

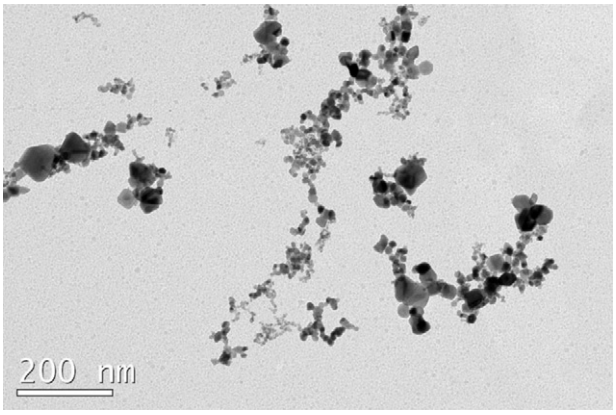

Fig. 1. TEM images of SnO_2 (JEOL JEM-101 FEG (100 kV) microscope) nanoparticles in ethylene glycol, at a concentration of 0.005% (v/v).

2. Experimental

2.1. Sample preparation and characterization

The SnO_2 nanofluid samples used in this work were prepared from tin(IV) oxide nanopowder supplied by Aldrich, with a declared diameter distribution $D < 100$ nm. Ethylene glycol provided also by Aldrich (99%) was used as base fluid. The nanoparticle powder was weighed using a Mettler AE-240 electronic balance, whose accuracy is 5×10^{-5} g. The powder was dispersed into a predetermined volume of the base fluid to obtain the desired weight percentage (up to 25 wt% for thermal conductivity and viscosity measurements and up to 5 wt% for density measurements). The estimated uncertainty for weight fractions was determined to be lower than 0.03%.

The morphology and size distribution of the SnO_2 nanoparticles in EG (0.005%, v/v) were studied by using the transmission electron microscopy (TEM) technique. The equipment used in this case was a JEOL JEM-101 FEG (100 kV) microscope. Fig. 1 shows the TEM image of the SnO_2 nanoparticles. It can be noted that the product is composed of quasi-spherical and rather polydisperse nanoparticles. The size distribution was estimated using IMAGETOOL freeware software, which was used to determine the diameters of a large number of particles in several images. In Fig. 2 the lognormal size distribution obtained is shown. The average diameter value computed using this method was $D = 17 \pm 9$ nm showing that the average size value provided by Aldrich was in this case very conservative.

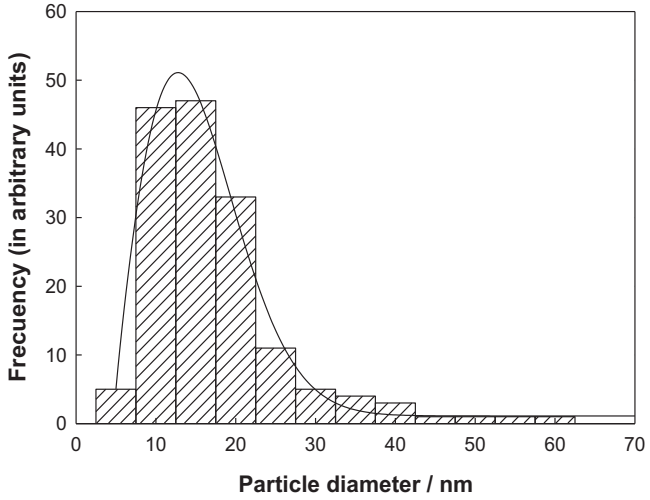

Fig. 2. Size distribution of SnO_2 nanoparticles in ethylene glycol (0.005%, v/v).

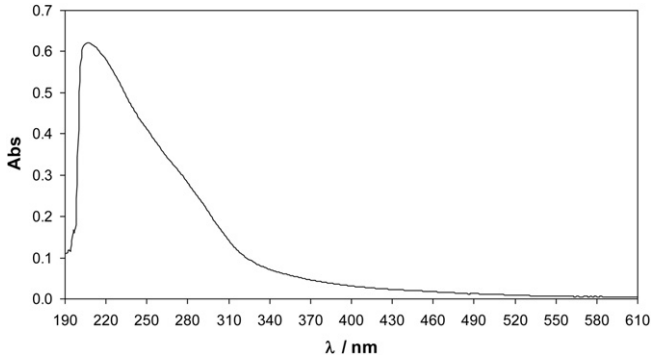

Fig. 3. UV–vis absorption spectrum of SnO_2/EG nanofluid, 0.01 wt%, T = 298.15 K.

The stability of the nanofluid was evaluated using a spectrometer Agilent HP 8453 UV-Vis equipped with a thermostated cell carrier. Fig. 3 shows a typical recording for the optical absorption spectrum of SnO_2/EG nanofluid. A wavelength value close to maximum was then fixed, and the absorbance time evolution for the sample at λ = 208 nm was analysed. The absorbance decrease in 24 h was found to be lower than 1%, indicating that the sample is stable and adequate for the type of measurements performed in this work, where the time from sample dispersion to the experimental measurements was very short. The samples were prepared by applying an Ultrasonic homogenizer probe (Bandelin Sonoplus 2200 HD), during 16 min. A discussion of the performance of different sonication methods has been presented in a previous work [21].

2.2. Measurements

After the adequate characterization of the sample, thermal conductivity, rheological behaviour and density of SnO_2 nanofluid samples were measured. Thermal conductivity was determined by a transient hot-wire method, which is one of the most accurate techniques to determine the thermal conductivity of fluids, including nanofluids, as pointed out by several authors [3,16]. Thermal conductivity data were measured using the Decagon Devices KD2 Pro Thermal Properties Analyser (Decagon Devices Inc., Pullman, WA, USA), whose principle of measurement is based on the transient hot-wire source approach. Heating the probe immersed in the sample while simultaneously monitoring its temperature evolution allows to calculate the fluid thermal conductivity, according to the model by Carslaw and Jaeger [22]. The uncertainty of the thermal conductivity measurement was estimated to be lower than 3%. More details about the measurement technique and its advantages were discussed in a previous work [4,5,23].

The rheological behaviour of the nanofluids was analysed using a Physica MCR 101 rheometer (Anton Paar, Austria). The equipment allows controlling torques between 0.1 μN m and 125 mN m, and normal force from 0.1 to 30 N. The cone-plate geometry with a cone diameter of 25 mm and a cone angle of 1° was used. All experiments are conducted at a constant gap value of 0.048 mm and an initial temperature stabilization period at 303.15 K using a Peltier system is always respected. Two types of experiments were carried out to investigate the nanofluid rheological behaviour. The first one is a non-linear viscoelastic experiment, usually referred to as flow curve, in which shear viscosity variation with shear rate is measured. The second type of experiment is a linear viscoelastic experiment (oscillatory), with the objective to determine the frequency-dependent energy of the storage modulus G' and loss modulus G''. The flow curves give information of relatively large deformations, whereas the storage and loss modulus reveal the mechanical properties of the material under small amplitude oscillatory shear.

Table 1
Experimental values of the thermal conductivity for SnO_2/EG nanofluids.

ϕ	κ/W m^{-1} K^{-1}		
	283.15 K	303.15 K	323.15 K
0.00000	0.239	0.243	0.247
0.00829	0.242	0.245	0.248
0.02754	0.259	0.262	0.265
0.04977	0.274	0.277	0.279

Densities were measured at different pressures and temperatures using an Anton Paar DMA 512P vibrating tube densimeter. The experimental procedure, calibration, temperature and pressure control were detailed in previous works [24,25]. The high pressure density uncertainty was estimated from the uncertainties of the reference substances used for calibration, water and vacuum in this case, following the procedure introduced by Lagourette et al. [26] and the influence of both temperature and pressure, and it was estimated to be lower than 10^{-4} g cm^{-3}. This vibrating tube densimeter calibration procedure has been widely used in literature (see e.g. Segovia et al. [27]).

3. Results and discussion

3.1. Thermal conductivity

Thermal conductivity of three different SnO_2/EG nanofluids samples were measured at 283.15 K, 303.15 K and 323.15 K. Experimental thermal conductivities, κ_{nf}, are presented in Table 1, as a function of volume fraction. The volume fractions, ϕ, were estimated from the densities of the pure base fluid (1.0176 g cm^{-3} at 303.15 K [4]) and the bulk solid oxide (6.95 g cm^{-3}, value provided by the manufacturer). As it can be observed in Fig. 4 the addition of tin(IV) oxide nanopowder increases the thermal conductivity of the nanofluid if compared with the base pure fluid. This enhancement (κ_{nf}/κ_0, where the subscripts *nf* and 0 refer to the nanofluid and base fluid, respectively), has been found to be almost temperature independent for a given concentration. Average enhancement values calculated lie between 1% at the lowest volume fraction and 14% for the highest concentration.

With the objective to estimate the thermal conductivity of the nanofluids, the classical Maxwell model [28], proposed for

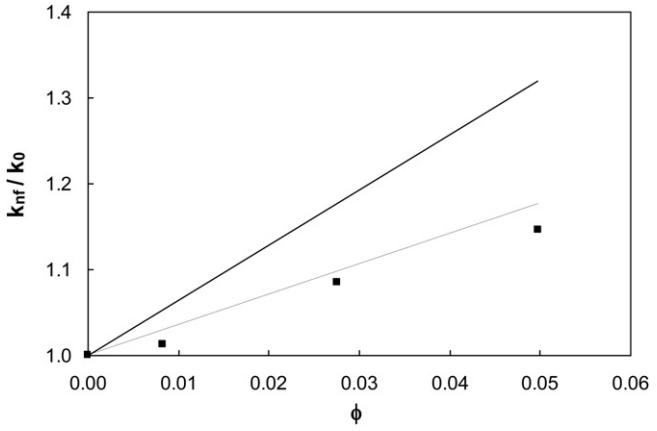

Fig. 4. Enhancement in the thermal conductivity (κ_{nf}/κ_0) at 283.15 K of SnO_2/EG nanofluids as a function of nanoparticle volume fraction. Experimental data (■). Solid line, prediction of Maxwell model (Eq. (1)); and dotted line, Turian model (Eq. (2)).

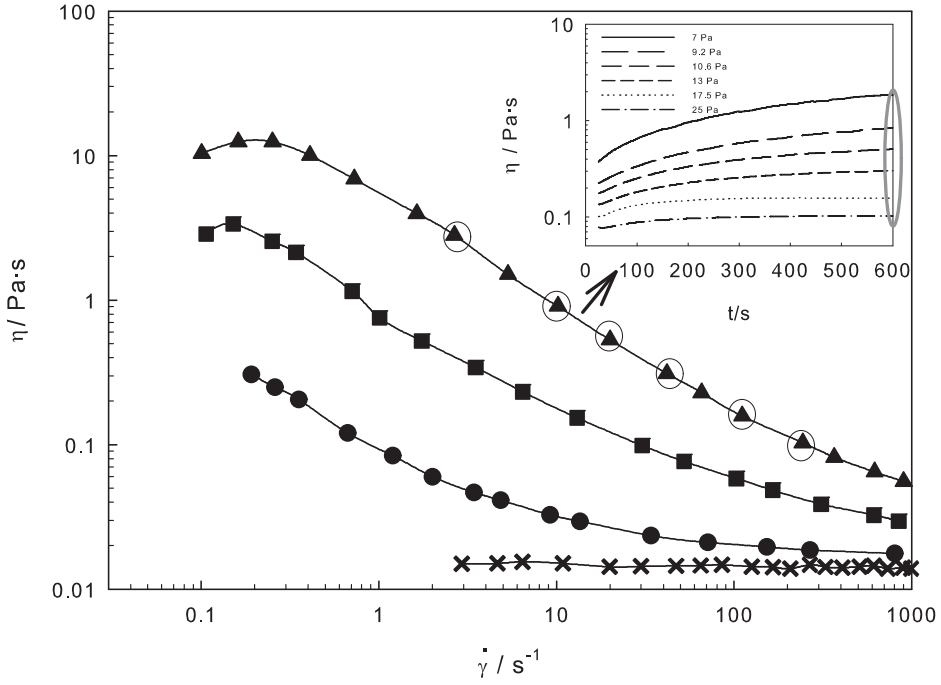

Fig. 5. Viscosity (η) versus shear rate ($\dot{\gamma}$) dependence of EG/SnO_2 nanofluids at 303.15 K and $t \geq 600$ s for different weight concentrations: (×) EG; (●) 5 wt%; (■) 15 wt%; (▲) 25 wt%. The inset shows viscosity versus time dependence for 25 wt% nanofluids at controlled shear stress.

homogeneous liquid/solid suspensions with relatively large and spherical particles, was applied:

$$\kappa_{nf} = \frac{\kappa_p + \kappa_0 + 2(\kappa_p - \kappa_0)\phi}{\kappa_p + \kappa_0 - 2(\kappa_p - \kappa_0)\phi}\kappa_0 \quad (1)$$

where κ_{nf}, κ_p and κ_0 refer to thermal conductivity of the nanofluid, solid particles and bulk liquid, respectively. ϕ stands for the particle volume fraction (vol.%). Tabulated values reported by Turkes et al. [29] were used for the thermal conductivity of the bulk tin dioxide with $\kappa_{SnO2} = 40\,W\,m^{-1}\,K^{-1}$ (polycrystalline). Many other models have been proposed based on the traditional Maxwell formulation, considering the influence of factors as particle diameter, surface area, shape, Brownian motion, or solid/fluid interfacial effects [30–34]. We also used our experimental thermal conductivity data to test the equation proposed by Turian et al. [35] to estimate the effective thermal conductivity:

$$\kappa_{nf} = \kappa_p^{\phi}\kappa_0^{(1-\phi)} \quad (2)$$

where

$$\kappa_p = \kappa_{bulk}(1 - e^{-A \cdot D}) \quad (3)$$

Eq. (3) takes into account the size dependence of nanoparticles [36,37], where κ_{bulk} is the bulk thermal conductivity of the solid at the temperature of interest, D is the average nanoparticle diameter (in nm), and $A = 0.01\,nm^{-1}$.

The experimental values of thermal conductivity, together with the predictions based on Eqs. (1) and (2) for the nanofluids studied are represented in Fig. 4 at 283.15 K. Similar results have been obtained for the other temperatures. Maxwell model over predicts in this case the experimental enhancement of the thermal conductivity (with and average percent deviation of 4.5%), while the Turian equation also over predicts the thermal conductivities, but the estimations are closer to our experimental data, with and overall average percent deviation of 2.3%.

3.2. Rheological behaviour

Fig. 5 shows the viscosity of pure ethylene glycol (EG) as a function of shear rate at 303.15 K from controlled shear stress tests. The torques applied started at the minimum value accessible to the rheometer used, 0.1 μN m, covering a wide range of shear rate (3–1000 s^{-1}). As shown in Fig. 5, the shear viscosity is independent of the shear rate for pure EG, evidencing a Newtonian behaviour. The flow curves of tin(IV) oxide nanofluids with particle weight concentrations of 5, 15 and 25% were measured and they are also shown in Fig. 5. The obtained curves indicate non-Newtonian behaviour (pseudo-plastic type) for all nanofluid samples. At the two higher concentrations a first Newtonian plateau with shear thinning appears in the lower shear rate region. It was not possible to detect this Newtonian plateau for the lower concentrations studied due to minimum shear rate value accessible to the rheometer used. The inset in Fig. 5 shows the time evolution of shear viscosity for some shear stress of the 25 wt% EG/SnO_2 sample, and its increase evidences rheopectic behaviour, or a structure gain under shear. For this reason, all flow curves were measured after the preliminary application of a constant stress to the sample during 600 s. This time evolution of viscosity had been reported in a previous work of our group for Fe_2O_3/EG nanofluids [15], but in that case the time evolution was the opposite, i.e. the nanofluid showed thixotropic behaviour. Any of these effects must be carefully considered when performing viscosity measurements of nanofluids, because it may produce spurious values or trends for the measured data. The effect of these trends on any practical application involving nanofluid flow must be outlined, and this dynamic evolution of viscosity may be considered as an evidence of the inherent complexity of this type of systems, whose rich behaviour is still far from being understood in the framework of colloid science theories.

For all concentrations, oscillatory or dynamic experiments were also carried out, in order to characterize the viscoelastic behaviour. The power of dynamic testing is that, by using the measured phase angle, the stress can be separated into two terms, namely elastic and viscous stress. The elastic or storage modulus, G', and the viscous

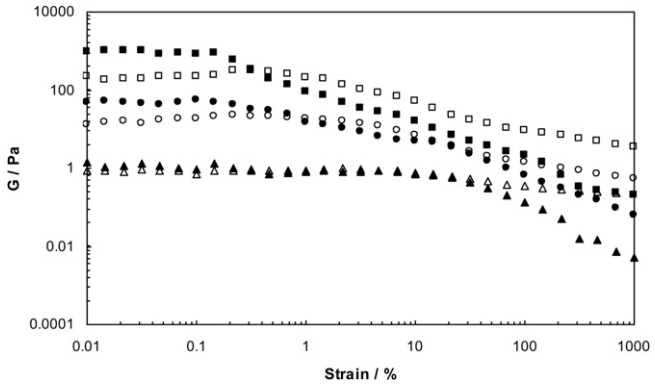

Fig. 6. Storage modulus (G', black symbols) and loss modulus (G'', white symbols) at 40 rad s^{-1} for SnO_2/EG nanofluids as a function of strain at 303.15 K for different concentrations: triangles: 5 wt%, circles: 15 wt% and squares: 25 wt%.

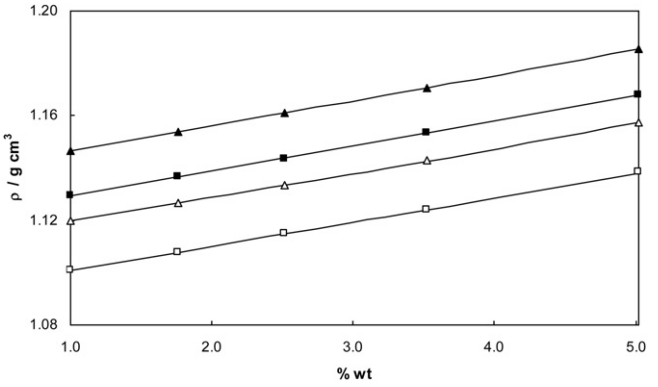

Fig. 8. Density (ρ) for SnO_2/EG nanofluids at different temperatures and pressures. Black symbols at 283.15 K and white symbols at 323.15 K. Squares: 0.1 MPa, and triangles: 45 MPa. The solid line represents the correlation with Tammann–Tait equation.

or loss modulus G'' can be calculated from the elastic and viscous stresses, respectively. First of all, to define the linear viscoelastic, strain sweep tests were performed at a constant frequency of 40 rad s^{-1}. The results obtained are shown in Fig. 6. It can be noted that all samples present a linear regime, in which storage modulus, G', and loss modulus, G'', are constant, and this linear region is concentration dependent with G' higher than G''. When the fluid structure is destroyed or disaggregation of nanoparticles occurs, G' and G'' decrease with the strain.

Frequency sweep tests, shown in Fig. 7, were also carried out at a constant strain value, 0.08%, which is inside the linear viscoelastic region. Overall the frequency range studied (600–10 rad s^{-1}), the storage modulus is also higher than the loss modulus, $G' > G''$, revealing that the elastic properties are dominant. Both modulus absolute values increase with nanoparticle concentrations for a given frequency.

3.3. Density

With the aim to characterize the volumetric behaviour of this nanofluid, experimental density measurements have been carried out at concentrations from 1% to 5% in weight fraction, and a pressure range from 0.1 to 45 MPa at the temperatures of 283.15, 303.15 and 323.15 K. Experimental results are plotted in Fig. 8. The trend shown with pressure and temperature is in concordance with the standard trend shown by the base fluid, as ρ decreases with increasing temperature and increases with pressure. The Tammann–Tait equation was employed to correlate the experimental density results.

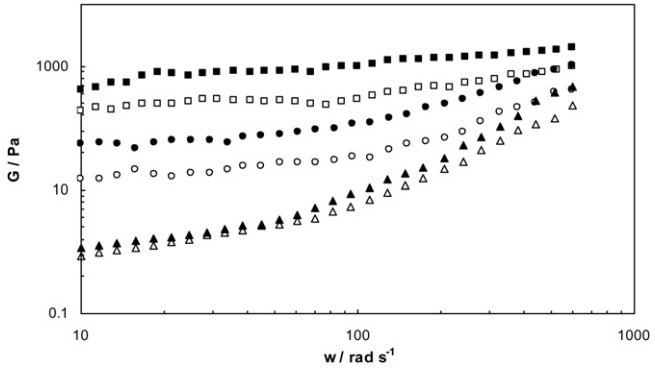

Fig. 7. Storage modulus (G', blacksymbols) and loss modulus (G'', white symbols) as a function of frequency for SnO_2/EG nanofluids at a constant strain of 0.08%, triangles: 5 wt%, circles: 15 wt% and squares: 25 wt%.

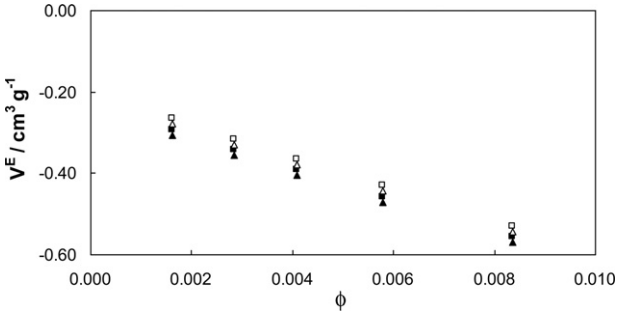

Fig. 9. Excess specific volume (V^E) for SnO_2/EG nanofluids at different temperatures and pressures. Black symbols: 283.15 K; white symbols: 323.15 K. Squares: experimental values at 0.1 MPa, and triangles: 45 MPa.

An analogy to fluid mixture non-ideality characterization can be established through the calculation of excess specific volume, calculated in this case on a mass basis according to the expression:

$$V^E = \frac{1}{\rho_{nf}} - \sum_{i=1}^{n} \frac{w_i}{\rho_i} \quad (4)$$

where w stands for mass fraction, n is the number of mixture components, and nf refers to the nanofluid. Fig. 9 shows a plot of these values at 283.15 K and 323.15 K, and at two pressures, 0.1 and 45 MPa. Although the values obtained from Eq. (4) do not correspond exactly to an excess property from a thermodynamic point of view, because nanoparticles and base fluid are not in the same state, the procedure was used previously to give an account of non-additivity of volume for these systems [4,38,39]. This noticeable volumetric deviation from ideal behaviour may be attributed to the interface effects on the bulk fluid properties produced by the solid nanoparticle surface, or even to the interactions among nanoparticles, which means that neglecting this type of interactions within a nanofluid can only be guessed as a first order approximation. These deviations from ideality increase with the concentration of nanoparticles and pressure while diminish when the temperature increases.

4. Conclusions

Thermal conductivities of tin(IV) oxide in ethylene glycol nanofluids have been determined experimentally as a function of volume concentration and temperature, and also density as a function of these variables and pressure. The rheological behaviour of these nanofluid samples has been studied at atmospheric

pressure and a single temperature. Enhancements up to 14% were found for thermal conductivity. The Maxwell model [28] and the equation proposed by Turian et al. [35] were applied to estimate thermal conductivities, finding that both method overpredict experimental values, although the explicit consideration of the average nanoparticle size in the second case improves estimations. The non-Newtonian nature of EG/SnO_2 nanofluids for different concentrations was demonstrated and it was found that these nanofluids samples show shear-thinning behaviour and rheopecty. The storage modulus, G', decreases after a certain critical strain, or the strain value where shear stress deviates from linear trend. The results of the frequency sweep experiment show that within the frequencies range studied in this work, the storage modulus is higher than the loss modulus, $G' > G''$, meaning that the elastic behaviour is dominant. The volumetric behaviour shows a significant contractive trend on mixing and a non-ideal volumetric behaviour, which is affected by concentration, and also but pressure, although the influence of this last variable is less important.

Acknowledgements

The authors acknowledge CACTI (Univ. deVigo) for technical assistance, Xunta de Galicia (grant PGIDIT07PXIB314181PR), and Min. de Ciencia e Innovación (Ramón y Cajal Program), all in Spain, for financial support. AM would like to acknowledge also financial support from CONICET in Argentina.

References

[1] S.K. Das, S.U.S. Choi, H.E. Patel, Heat Transf. Eng. 27 (10) (2006) 3–19.
[2] Y. Li, J.E. Zhou, S. Tung, E. Schneider, S. Xi, Powder Technol. 196 (2) (2009) 89–101.
[3] S.M.S. Murshed, K.C. Leong, C. Yang, Appl. Therm. Eng. 28 (17–18) (2008) 2109–2125.
[4] M.J. Pastoriza-Gallego, L. Lugo, J.L. Legido, M.M. Piñeiro, J. Appl. Phys. 110 (1) (2011) 014309.
[5] M.J. Pastoriza-Gallego, L. Lugo, J.L. Legido, M.M. Piñeiro, Nanoscale Res. Lett. 6 (1) (2011) 221.
[6] J. Philip, P.D. Shima, B. Raj, Appl. Phys. Lett. 92 (4) (2008) 043108.
[7] E.V. Timofeeva, A.N. Gavrilov, J.M. Mccloskey, Y.V. Tolmachev, S. Sprunt, L.M. Lopatina, J.V. Selinger, Phys. Rev. E 76 (6) (2007) 061203.
[8] S.U.S. Choi, Z.G. Zhang, P. Keblinski, Nanofluids, vol. 6, Scientific Publishers, New York, 2004, pp. 757–773.
[9] L. Wang, J. Fan, Nanoscale Res. Lett. 5 (8) (2010) 1241–1252.
[10] S. Zussman, New Nanofluids Increase Heat Transfer Capability, Argonne National Laboratory, USA, 1997, p. 4.
[11] H. Chen, Y. Ding, A. Lapkin, X. Fan, J. Nanopart. Res. 11 (6) (2009) 1513–1520.
[12] H. Chen, Y. Ding, C. Tan, New J. Phys. 9 (2007) 367.
[13] J. Chevalier, O. Tillement, F. Ayela, Appl. Phys. Lett. 91 (23) (2007) 233103.
[14] D.R. Heine, M.K. Petersen, G.S. Grest, J. Chem. Phys. 132 (18) (2010) 184509.
[15] M.J. Pastoriza-Gallego, L. Lugo, J.L. Legido, M.M. Piñeiro, Nanoscale Res. Lett. 6 (2011) 560.
[16] J. Buongiorno, D.C. Venerus, N. Prabhat, T. Mckrell, J. Townsend, R. Christianson, Y.V. Tolmachev, P. Keblinski, L.-W. Hu, J.L. Alvarado, I.C. Bang, S.W. Bishnoi, M. Bonetti, F. Botz, A. Cecere, Y. Chang, G. Chen, H. Chen, S.J. Chung, M.K. Chyu, S.K. Das, R. Di Paola, Y. Ding, F. Dubois, G. Dzido, J. Eapen, W. Escher, D. Funfschilling, Q. Galand, J. Gao, P.E. Gharagozloo, K.E. Goodson, J.G. Gutierrez, H. Hong, M. Horton, K.S. Hwang, C.S. Iorio, S.P. Jang, A.B. Jarzebski, Y. Jiang, L. Jin, S. Kabelac, A. Kamath, M.A. Kedzierski, L.G. Kieng, C. Kim, J.-H. Kim, S. Kim, S.H. Lee, K.C. Leong, I. Manna, B. Michel, R. Ni, H.E. Patel, J. Philip, D. Poulikakos, C. Reynaud, R. Savino, P.K. Singh, P. Song, T. Sundararajan, E. Timofeeva, T. Tritcak, A.N. Turanov, S. Van Vaerenbergh, D. Wen, S. Witharana, C. Yang, W.-H. Yeh, X.-Z. Zhao, S.-Q. Zhou, J. Appl. Phys. 106 (9) (2009) 094312.
[17] H. Ahmari, S.G. Etemad, Rheol. Acta 48 (2) (2009) 217–220.
[18] I.M.G. Dos Santos, A.G. De Souza, F.R. Sensato, E.R. Leite, E. Longo, J.A. Varela, J. Eur. Ceram. Soc. 22 (8) (2002) 1297–1306.
[19] S. Habibzadeh, A. Kazemi-Beydokhti, A.A. Khodadadi, Y. Mortazavi, S. Omanovic, M. Shariat-Niassar, Chem. Eng. J. 156 (2) (2010) 471–478.
[20] R.S. Vajjhaa, D.K. Dasa, B.M. Mahagaonkar, Pet. Sci. Technol. 27 (6) (2009) 612–624.
[21] M.J. Pastoriza-Gallego, C. Casanova, R. Páramo, B. Barbés, J.L. Legido, M.M. Piñeiro, J. Appl. Phys. 106 (6) (2009) 064301.
[22] Carslaw Hs, J. Jc, Conduction of Heat in Solids, vol. 25, Oxford University Press, London, 1959.
[23] D. Cabaleiro, M.J. Pastoriza-Gallego, M.M. Piñeiro, J.L. Legido, L. Lugo, J. Chem. Thermodyn. 50 (2012) 80–88.
[24] M.M. Piñeiro, D. Bessières, J.M. Gacio, H. Saint-Guirons, J.L. Legido, Fluid Phase Equilib. 220 (1) (2004) 127–136.
[25] M.M. Piñeiro, D. Bessières, J.L. Legido, H. Saint-Guirons, Int. J. Thermophys. 24 (5) (2003) 1265–1276.
[26] B. Lagourette, C. Boned, H. Saint-Guirons, H.Z.P. Xans, B. Lagourette, C. Boned, H. Saint-Guirons, P. Xans, H. Zhou, Meas. Sci. Technol. 3 (1992) 699–703.
[27] J.J. Segovia, O. Fandiño, E.R. López, L. Lugo, M.C. Martín, J. Fernández, J. Chem. Thermodyn. 41 (2009) 632–638.
[28] J.C. Maxwell, A Treatise on Electricity and Magnetism, Oxford University Press, London, 1892.
[29] P. Turkes, C. Pluntke, R. Helbig, J. Phys. C 13 (26) (1980) 4941–4951.
[30] R.L. Hamilton, O.K. Crosser, Ind. Eng. Chem. Fundam. 1 (3) (1962) 187.
[31] R. Prasher, P. Bhattacharya, P.E. Phelan, Phys. Rev. Lett. 94 (2) (2005) 025901.
[32] X.-Q. Wang, A.S. Mujumdar, Int. J. Therm. Sci. 46 (1) (2007) 1–19.
[33] W. Yu, S.U.S. Choi, J. Nanopart. Res. 5 (1–2) (2003) 167–171.
[34] S.M.S. Murshed, K.C. Leong, C. Yang, Int. J. Therm. Sci. 47 (5) (2008) 560–568.
[35] R.M. Turian, D.J. Sung, F.L. Hsu, Fuel 70 (10) (1991) 1157–1172.
[36] M.P. Beck, Y. Yuan, P. Warrier, A.S. Teja, J. Nanopart. Res. 11 (5) (2009) 1129–1136.
[37] A.S. Teja, M.P. Beck, Y. Yuan, P. Warrier, J. Appl. Phys. 107 (11) (2010) 114319.
[38] M.J. Pastoriza-Gallego, C. Casanova, J.L. Legido, M.M. Piñeiro, Fluid Phase Equilib. 300 (1–2) (2011) 188–196.
[39] C. Wei, Z. Nan, X. Wang, Z. Tan, J. Chem. Eng. Data 55 (7) (2010) 2524–2528.